

## Electromagnetic circulatory forces and rotordynamic instability in electric machines

Holopainen TP <sup>a</sup>, Tenhunen A <sup>b</sup> and Arkkio A <sup>b</sup>

<sup>a</sup> *VTT Industrial Systems, Technical Research Centre of Finland, P.O. Box 1705, FIN-02044 VTT, Finland*

<sup>b</sup> *Laboratory of Electromechanics, Helsinki University of Technology, P.O. Box 3000, FIN-02015 HUT, Finland*

The electromechanical interaction in electric machines induces additional forces between the rotor and stator. To study this interaction, a simple electromechanical model was developed. The mechanical behaviour was modelled by the Jeffcott rotor. The electromagnetic forces were described by a simple parametric model including two electromagnetic variables. The aim of the study was to investigate the effects of electromechanical interaction on rotordynamic instability in electric motors. If the new electromagnetic variables are interpreted as ‘quasi-displacements’, the interaction turns up in the equations of motion as additional damping, stiffness and circulatory terms. The electromagnetically induced damping and stiffness effects in electric motors have been studied previously. However, the effects of circulatory terms have been overridden in electric motors. It is well-known that the circulatory, i.e. cross-coupled stiffness, terms are a major source of instability in rotating machines. Thus, the presented model offers a new and simple explanation for the rotordynamic instability in electric motors. The numerical examples raised another source of instability. The system parameters may yield a negative-definite stiffness matrix (symmetric part), which destabilize the system without stabilizing forces.

**Keywords:** Rotors, stability analysis, circulatory force, electromechanical interaction, electric machines.

### 1. Introduction

An electric motor converts electric energy to mechanical one. The magnetic field in the air gap of the machine generates the tangential forces required for the torque generation. In addition, the field produces other force components that interact with the machine structures and may excite harmful vibrations. At relatively low frequencies, the vibration amplitudes may be large enough to couple the electromagnetic system with the mechanical one. This electromechanical interaction changes the vibration characteristics of the machine, e.g., it may induce additional damping or cause rotordynamic instability.

Früchtenicht, Jordan and Seinsch [1] developed an analytic model for the electromechanical forces between the rotor and stator, when the rotor is in circular whirling motion. Using this model and assuming synchronous whirling motion, they determined the stiffness and damping coefficients induced by the electromagnetic field. Belmans, Vandepuut and Geysen [2] investigated analytically and experimentally the flexible-shaft induction motors. Their calculation model resembled to that of Früchtenicht et al. [1], but they focused on the two-pole machines. They concluded that one potential reason for the rotordynamic instability results from the electromagnetic damping coefficient which may be negative. Skubov and Shumakovich [3] developed an analytic electromechanical model and studied the rotordynamic instability. They found out that the tangential component of the electromagnetic total force may be the reason for the instability. Arkkio et al. [4] presented a simple parametric force model for the electromagnetic forces acting between the rotor and stator when the rotor is in whirling motion. The model parameters of an electric motor were determined by numerical simulations including the non-linear saturation of magnetic materials. The numerical results were validated by extensive measurements.

Previous research on this issue has not been conclusive, in part because it has generally been based on the assumption of synchronous whirling motion [1,2], and in part because the effects of saturation of magnetic materials are not included in the analytical force models used previously [1,2,3]. In present study, we rejected the assumption of synchronous whirling motion and used as the starting point the numerical simulations of electromagnetic fields. The aim of this study was to investigate the effects of electromechanical interaction on rotordynamic instability in electric motors.

In this study, we develop an analytical model to study the electromechanical interaction and stability. The Jeffcott

rotor model is combined with the parametric force model. The coupled equations of motion are transformed into a non-dimensional form. Using this simple model, numerical results describing the effects of electromechanical interaction are calculated. The vibration characteristics of the system are investigated by the eigenvalue analysis. The rotordynamic stability is studied by using the modified Bilharz schema [5]. This yields four necessary and sufficient criteria for the stability of the system. Some of the criteria can be studied in analytical form. The rest of the criteria can be studied numerically.

## 2. Nomenclature

$a_{p\pm 1}$	= electromagnetic force parameters	$\mathbf{q}$	= vector of variables in second order model
$c_i$	= coefficients of characteristic polynomial	$\mathbf{u}_r$	= eigenvector $r$
$d$	= mechanical damping coefficient	$\mathbf{x}$	= vector of variables in first order model
$f$	= excitation force	$\mathbf{A}$	= system matrix
$j$	= imaginary unit	$\mathbf{B}$	= coefficient matrix for input
$k$	= shaft stiffness coefficient	$\mathbf{C}$	= damping matrix
$k_e$	= effective stiffness coefficient	$\mathbf{H}$	= circulatory matrix
$k_0$	= electromagnetic force parameter	$\mathbf{I}$	= identity matrix
$k_{p\pm 1}$	= electromagnetic force parameters	$\mathbf{K}$	= stiffness matrix
$m$	= mass of the rotor	$\mathbf{M}$	= mass matrix
$p$	= number of pole pairs of the motor	$\mathbf{Q}$	= loading vector
$q_{p\pm 1}$	= electromagnetic field variables	$\delta''$	= radial air-gap length
$r_{ij}$	= term $ij$ in recursive schema	$\delta_r$	= decay constant of eigenvector $r$
$s$	= Laplace variable	$\tau$	= non-dimensional time
$s_0$	= machine slip	$\omega$	= angular frequency
$t$	= time	$\omega_n$	= natural frequency of mechanical system
$x, y$	= co-ordinates	$\omega_0$	= supply frequency
$z$	= complex variable	$\Omega$	= rotor angular frequency
$D_i$	= Bilharz determinant $i$	$\tilde{a}$	= non-dimensional form of $a$
$F_{em}$	= electromagnetic total force	$a_{\text{Im}}$	= imaginary part of $a$
$K$	= transfer function	$a_{\text{Re}}$	= real part of $a$
		$\bar{a}$	= complex conjugate of $a$
		$\dot{a}$	= differentiation of $a$ with respect to time
		$a_{,\tau}$	= differentiation of $a$ with respect to $\tau$

## 3. Method of analysis

### 3.1 Rotor model

To model the mechanical behaviour of the system, we apply the Jeffcott rotor which is a thin unbalanced disk located at the middle of a uniform, massless, flexible shaft. The shaft is simply supported at its ends by rigid frictionless bearings. We assume a damping force from the surrounding medium of viscous type. In Jeffcott model, the disc is assumed to move only in its own plane, or more precisely in  $xy$ -plane. The origin of this plane is assumed to coincide with the rotation axis and define the center position by a complex variable

$$z(t) = x(t) + jy(t) \quad (1)$$

The equation of motion of this rotor using the complex co-ordinates approach can be written [6]

$$m\ddot{z} + d\dot{z} + kz = f(t) \quad (2)$$

where  $m$  is the mass of the disc,  $d$  is the coefficient for the non-rotating damping,  $k$  is the shaft stiffness coefficient, and  $f$  is the excitation force, e.g., due to the mass unbalance.

### 3.2 Force model

Arkkio et al. [4] presented a low order linear model for the electromagnetic forces between the rotor and stator. The proposed transfer function model can be written in complex form as

$$F_{em}(s) = K(s)z(s) \quad (3)$$

where  $F_{em}$  is the complex valued electromagnetic force exerted on the rotor,  $z$  is the complex valued displacement of the rotor center,  $s$  is Laplace variable, and  $K(s)$  is a second order transfer function

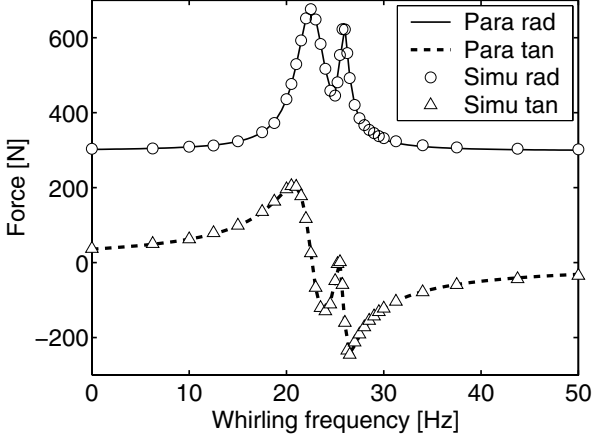


Figure 1. The radial and tangential forces as function of the whirling frequency. The discrete points represent the simulation results and the curves are obtained by a curve fitting procedure together with the parametric model. [4]

Figure 1 shows the radial and tangential force components as a function of whirling frequency. The 15 kW four-pole cage induction motor is loaded by the rated torque and supplied by the rated voltage. The whirling radius is 11 % of the radial air-gap length. The radial component is defined in the direction of the shortest air gap and the tangential component perpendicular to the radial one.

The linear second order transfer function (4) corresponds to the equations

$$\begin{aligned} \dot{q}_{p-1} &= a_{p-1}q_{p-1} + k_{p-1}z(t) \\ \dot{q}_{p+1} &= a_{p+1}q_{p+1} + k_{p+1}z(t) \\ F_{em}(t) &= q_{p-1} + q_{p+1} + k_0z(t) \end{aligned} \quad (6)$$

where  $q_{p-1}$  and  $q_{p+1}$  are new variables related to the eccentricity harmonics  $p-1$  and  $p+1$  of the air-gap field.

### 3.3 Combined model

The electromechanical rotor equations are obtained by combining the mechanical equations of motion (2) with the equations of electromagnetic forces (6). Thus, the coupled system of equations can be written

$$\begin{aligned} m\ddot{z} + d\dot{z} + (k - k_0)z - q_{p-1} - q_{p+1} &= f(t) \\ \dot{q}_{p-1} &= a_{p-1}q_{p-1} + k_{p-1}z \\ \dot{q}_{p+1} &= a_{p+1}q_{p+1} + k_{p+1}z \end{aligned} \quad (7)$$

### 3.4 Model in non-dimensional form

The system of equations (7) can be transformed into a non-dimensional form employing new non-dimensional variables

$$\begin{aligned} \tilde{z} &= \frac{z}{\delta^n} & \tau &= \frac{t\omega_0}{p} & \tilde{q}_{p\pm 1} &= \frac{p^2}{\delta^n \omega_0^2 m} \cdot q_{p\pm 1} \end{aligned} \quad (8)$$

$$K(s) = k_0 + \frac{k_{p-1}}{s - a_{p-1}} + \frac{k_{p+1}}{s - a_{p+1}} \quad (4)$$

where  $k_0$ ,  $k_{p-1}$ ,  $k_{p+1}$ ,  $a_{p-1}$ , and  $a_{p+1}$  are the parameters of the model. The subscripts of the parameters  $p-1$  and  $p+1$  refer to the respective eccentricity harmonics of the electromagnetic fields. The parameter  $p$  refers to the number of pole pairs of the machine. The parameters  $k_{p\pm 1}$  and  $a_{p\pm 1}$  are generally complex valued. The imaginary parts of the latter pair of parameters can be written

$$a_{p\pm 1} = a_{p\pm 1, \text{Re}} + \left[1 - s_0(1 \pm p)\right] \frac{\omega_0}{p} \quad (5)$$

where  $s_0$  is the slip of rotor with respect to the fundamental harmonic, and  $\omega_0$  is the angular frequency of fundamental harmonic.

Arkkio et al. [4] determined the force parameters of an electric motor by calculating the electromagnetic forces induced by circular whirling motion ( $s = j\omega$ ). Figure 1

shows the radial and tangential force components as a function of whirling frequency. The 15 kW four-pole cage induction motor is loaded by the rated torque and supplied by the rated voltage. The whirling radius is 11 % of the radial air-gap length. The radial component is defined in the direction of the shortest air gap and the tangential component perpendicular to the radial one.

The linear second order transfer function (4) corresponds to the equations

$$\begin{aligned} \dot{q}_{p-1} &= a_{p-1}q_{p-1} + k_{p-1}z(t) \\ \dot{q}_{p+1} &= a_{p+1}q_{p+1} + k_{p+1}z(t) \\ F_{em}(t) &= q_{p-1} + q_{p+1} + k_0z(t) \end{aligned} \quad (6)$$

where  $q_{p-1}$  and  $q_{p+1}$  are new variables related to the eccentricity harmonics  $p-1$  and  $p+1$  of the air-gap field.

### 3.3 Combined model

The electromechanical rotor equations are obtained by combining the mechanical equations of motion (2) with the equations of electromagnetic forces (6). Thus, the coupled system of equations can be written

$$\begin{aligned} m\ddot{z} + d\dot{z} + (k - k_0)z - q_{p-1} - q_{p+1} &= f(t) \\ \dot{q}_{p-1} &= a_{p-1}q_{p-1} + k_{p-1}z \\ \dot{q}_{p+1} &= a_{p+1}q_{p+1} + k_{p+1}z \end{aligned} \quad (7)$$

### 3.4 Model in non-dimensional form

The system of equations (7) can be transformed into a non-dimensional form employing new non-dimensional variables

$$\begin{aligned} \tilde{z} &= \frac{z}{\delta^n} & \tau &= \frac{t\omega_0}{p} & \tilde{q}_{p\pm 1} &= \frac{p^2}{\delta^n \omega_0^2 m} \cdot q_{p\pm 1} \end{aligned} \quad (8)$$

where  $\delta''$  is the radial air-gap length. Employing these variables, the system equations can be written in non-dimensional form

$$\begin{aligned}\tilde{z}_{,\tau\tau} + \tilde{d}\tilde{z}_{,\tau} + \tilde{k}_e\tilde{z} - \tilde{q}_{p-1} - \tilde{q}_{p+1} &= \tilde{f}(\tau) \\ \tilde{q}_{p-1,\tau} &= \tilde{a}_{p-1}\tilde{q}_{p-1} + \tilde{k}_{p-1}\tilde{z} \\ \tilde{q}_{p+1,\tau} &= \tilde{a}_{p+1}\tilde{q}_{p+1} + \tilde{k}_{p+1}\tilde{z}\end{aligned}\quad (9)$$

where  $\tilde{k}_e = \tilde{k} - \tilde{k}_0$  is the effective stiffness coefficient, and the subscript  $\tau$  after comma refers to the differentiation with respect to non-dimensional time. The new non-dimensional parameters are

$$\begin{aligned}\tilde{d} &= \frac{pd}{m\omega_0} & \tilde{k} &= \frac{p^2k}{m\omega_0^2} & \tilde{k}_0 &= \frac{p^2k_0}{m\omega_0^2} & \tilde{k}_{p\pm 1} &= \frac{p^3k_{p\pm 1}}{m\omega_0^3} \\ \tilde{a}_{p\pm 1} &= \frac{pa_{p\pm 1}}{\omega_0} & \tilde{\Omega} &= \frac{p\Omega}{\omega_0} = 1 - s_0 & \tilde{\omega}_n &= \frac{p\omega_n}{\omega_0} & \tilde{f}(\tau) &= \frac{p^2}{m\delta''\omega_0^2} f(t)\end{aligned}\quad (10)$$

where  $\omega_n = \sqrt{k/m}$  is the natural mechanical frequency of the rotor, and  $\Omega$  is the angular frequency of the rotor.

### 3.5 Matrix representation

Using the complex formulation, Equations (9) can be written in matrix form

$$\mathbf{M}\ddot{\mathbf{q}} + \mathbf{C}\dot{\mathbf{q}} + (\mathbf{K} + \mathbf{H})\mathbf{q} = \mathbf{Q}\quad (11)$$

where  $\mathbf{q}$  is the vector of complex variables,  $\mathbf{M}$ ,  $\mathbf{C}$ ,  $\mathbf{K}$ , and  $\mathbf{H}$  are the mass, damping, stiffness, and circulatory matrices, respectively, and  $\mathbf{Q}$  is the loading vector. The matrices can be written explicitly

$$\mathbf{M} = \begin{bmatrix} 1 & 0 & 0 \\ 0 & 0 & 0 \\ 0 & 0 & 0 \end{bmatrix} \quad \mathbf{C} = \begin{bmatrix} \tilde{d} & 0 & 0 \\ 0 & 1 & 0 \\ 0 & 0 & 1 \end{bmatrix}\quad (12)$$

$$\mathbf{K} = \begin{bmatrix} \tilde{k}_e & \frac{-1 - \tilde{k}_{p-1}}{2} & \frac{-1 - \tilde{k}_{p+1}}{2} \\ \frac{-1 - \tilde{k}_{p-1}}{2} & -\tilde{a}_{p-1, \text{Re}} & 0 \\ \frac{-1 - \tilde{k}_{p+1}}{2} & 0 & -\tilde{a}_{p+1, \text{Re}} \end{bmatrix} \quad \mathbf{H} = \begin{bmatrix} 0 & \frac{-1 + \tilde{k}_{p-1}}{2} & \frac{-1 + \tilde{k}_{p+1}}{2} \\ \frac{1 - \tilde{k}_{p-1}}{2} & -j[1 - s_0(1 - p)] & 0 \\ \frac{1 - \tilde{k}_{p+1}}{2} & 0 & -j[1 - s_0(1 + p)] \end{bmatrix}$$

where the complex conjugate of a complex number  $z$  is denoted by  $\bar{z}$ . The mass, damping and stiffness matrices are Hermitian matrices, and the circulatory matrix is skew-Hermitian matrix. The Hermitian and skew-Hermitian matrices are generalizations of the real valued symmetric and skew-symmetric matrices, respectively. If the new electromagnetic variables  $\tilde{q}_{p\pm 1}$  are interpreted as ‘quasi-displacements’, the electromechanical interaction turns up in the equations of motion as additional damping, stiffness and circulatory terms. The circulatory, i.e. cross-coupled, stiffness terms induce circulatory forces, which can stabilize or destabilize the system [7]. In rotating machines, the circulatory forces are the major source of instability acting tangentially to the shaft whirl orbit and may consequently feed energy into the whirling motion [8].

### 3.6 First order model

To explore the system characteristics, the equations are transformed into the form of state equations. These equations can be written in the matrix form

$$\mathbf{x}_{\tau} = \mathbf{A}\mathbf{x} + \mathbf{B}\tilde{f}(\tau), \quad \mathbf{A} = \begin{bmatrix} 0 & 1 & 0 & 0 \\ -\tilde{k}_e & -\tilde{d} & 1 & 1 \\ \tilde{k}_{p-1} & 0 & \tilde{a}_{p-1} & 0 \\ \tilde{k}_{p+1} & 0 & 0 & \tilde{a}_{p+1} \end{bmatrix}, \quad \mathbf{x} = \begin{Bmatrix} \tilde{z} \\ \dot{\tilde{z}} \\ \tilde{q}_{p-1} \\ \tilde{q}_{p+1} \end{Bmatrix}, \quad \mathbf{B} = \begin{Bmatrix} 0 \\ 1 \\ 0 \\ 0 \end{Bmatrix} \quad (13)$$

The homogeneous part of these equations comprise the eigenvalue problem

$$[\mathbf{A} - \lambda\mathbf{I}]\mathbf{u} = \mathbf{0} \quad (14)$$

where  $\mathbf{I}$  is the identity matrix. The solution consists of 4 eigenvalues  $\lambda_r$  and associated eigenvectors  $\mathbf{u}_r$  ( $r = 1, 2, 3, 4$ ). These eigenvalues can be expressed in the general form

$$\lambda_r = -\delta_r + j\omega_r \quad (15)$$

where  $\delta_r$  is the decay constant, and  $\omega_r$  the frequency of the  $r$  th eigenvalue. The system is asymptotically stable, if all the eigenvalues have positive decay constant.

### 3.7 Stability criterion

To study the stability of the system, we apply the criterion presented by Parks and Hahn [5] for linear differential equations with complex coefficients. This criterion resembles the criterion developed by Bilharz [9], which is a generalization of the better-known Routh criterion for equations with complex coefficients. The characteristic equation of the system (14) can be written

$$\det[\mathbf{A} - \lambda\mathbf{I}] = \lambda^4 + c_3\lambda^3 + c_2\lambda^2 + c_1\lambda + c_0 = 0 \quad (16)$$

where  $c_i$  are the complex coefficients, and  $\lambda$  is an eigenvalue of the system. For this characteristic equation, a scheme can be written in matrix form

$$\begin{array}{ccccc} 1 & c_{3,\text{Im}} & -c_{2,\text{Re}} & -c_{1,\text{Im}} & c_{0,\text{Re}} \\ c_{3,\text{Re}} & c_{2,\text{Im}} & -c_{1,\text{Re}} & -c_{0,\text{Im}} & 0 \\ r_{31} & r_{32} & r_{33} & r_{34} & 0 \\ \vdots & \vdots & \vdots & 0 & 0 \end{array} \quad (17)$$

where the suffix Re or Im in the subscript denotes the real or imaginary part of the complex coefficients, respectively, and the recursive formula for the additional terms is

$$r_{ij} = \frac{r_{i-1,j+1} r_{i-2,j+1} - r_{i-2,j+1} r_{i-1,j+1}}{r_{i-1,j+1}} \quad (18)$$

The Bilharz determinants can be calculated from the elements of the first column

$$D_1 = r_{12} \quad D_2 = r_{13}r_{14}D_1 \quad D_3 = r_{15}r_{16}D_2 \quad D_4 = r_{17}r_{18}D_3 \quad (19)$$

and the criterion for asymptotic stability of the system is

$$D_i > 0, \quad i = 1, 2, 3, 4 \quad (20)$$

The first criterion can be written explicitly

$$D_1 = \tilde{d} - \tilde{a}_{p-1,\text{Re}} - \tilde{a}_{p+1,\text{Re}} > 0 \quad (21)$$

This criterion sets a combined condition for the mechanical damping and for two electromagnetic parameters, which are associated with the attenuation of the rotor currents. If we assume that the mechanical damping is zero, i.e.  $\tilde{d} = 0$ , we obtain from the second criterion

$$\tilde{k}_{p-1,\text{Re}} + \tilde{k}_{p+1,\text{Re}} > \frac{\tilde{a}_{p-1,\text{Re}} \tilde{a}_{p+1,\text{Re}} \left[ 4s_0^2 p^2 + (\tilde{a}_{p-1,\text{Re}} + \tilde{a}_{p+1,\text{Re}})^2 \right]}{\tilde{a}_{p-1,\text{Re}} + \tilde{a}_{p+1,\text{Re}}} \quad (22)$$

This criterion sets the lower limit for the sum of parameters  $\tilde{k}_{p\pm 1,\text{Re}}$  in terms of parameters  $\tilde{a}_{p\pm 1,\text{Re}}$ ,  $s_0$  and  $p$ . The third and fourth criteria are more complicated in explicit form, and their implications are more difficult to understand.

## 4. Results

### 4.1 The studied motor

The studied motor was a 15 kW four-pole cage induction motor. Arkkio et al. [4] used this motor as an example for extensive numerical simulations of electromagnetic forces. Their calculation results are verified by measurements, where the rotor is suspended by magnetic bearings. The electromagnetic force parameters are identified by curve fitting procedure assuming either real or complex  $k_{p\pm 1}$  parameters. The complex fitting procedure yields slightly better results. However, for the sake of simplicity, we applied here only real valued parameters for  $k_{p\pm 1}$ . We studied the motor operating at its rated power (15 kW), supplied by the rated voltage (380 V), and the rotor is running at the rated slip (0.032). All the parameters used in the calculations are given in Table 1. The stiffness, mass and damping properties of the rotor are roughly estimated.

### 4.2 Vibration characteristics of the studied motor

The natural bending frequency of the rotor without electromagnetic effects is 355.9 Hz. Table 2 shows the eigenvalue frequencies and decay constants of the electromechanical rotor system without mechanical damping. The two lowest modes are associated with the eccentricity harmonics of electromagnetic fields, and the two higher modes are associated with the forward (FW) and backward (BW) whirling modes. However, all modes have electromagnetic and mechanical contributions. The effect of electromechanical coupling on the whirling frequencies and their decay constants is minor. The frequencies of electromagnetic modes correspond to the frequencies of the eccentricity harmonics of electromagnetic fields. The decay constants of these modes are associated with the attenuation of rotor currents.

We note that in the studied motor the ratio of fundamental frequency, without electromagnetic effects, to the operating shaft speed is large ( $\omega_n/\Omega \approx 15$ ). This is typical for small electric motors. The electromechanical interaction is apparently more pronounced in motors having the ratio close to unit. This is usually the case in large electric motors. To study the electromechanical interaction we retained the electromagnetic properties of the motor but assumed that the shaft stiffness is lower than in the actual motor. A similar approach was employed by Früchtenicht et al. [1] and Belmans et al. [2] in their experimental investigations.

Table 1

Electromagnetic force parameters in non-dimensional form of a 15 kW induction motor [4]

Dimensional			Non-dimensional	
Symb.	Value	Unit	Symb.	Value
$\omega_0$	$2\pi \cdot 50$	rad/sec		
$m$	30	kg		
$\delta''$	$0.45 \cdot 10^{-3}$	m		
$p$	2			
$s_0$	0.032		$s_0$	0.032
$k_0$	$6.22 \cdot 10^6$	N/m	$\tilde{k}_0$	8.403
$k_{p-1}$	$15.7 \cdot 10^6$	N-rad/m-sec	$\tilde{k}_{p-1}$	0.1350
$k_{p+1}$	$74.9 \cdot 10^6$	N-rad/m-sec	$\tilde{k}_{p+1}$	0.6442
$a_{p-1,\text{Re}}$	-3.1	rad/sec	$\tilde{a}_{p-1,\text{Re}}$	-0.0200
$a_{p+1,\text{Re}}$	-10.6	rad/sec	$\tilde{a}_{p+1,\text{Re}}$	-0.0672
$k$	$1.5 \cdot 10^8$	N/m	$\tilde{k}$	203
$d$	$2 \cdot 10^3$	kg/sec	$\tilde{d}$	0.42

Table 2

The eigenvalues of the studied motor

Mode	Freq. [Hz]	Decay constant	Description
1	22.6	0.068	Mode $p+1$
2	25.8	0.021	Mode $p-1$
3	348.7	0.0025	FW whirling
4	348.7	0.0022	BW whirling

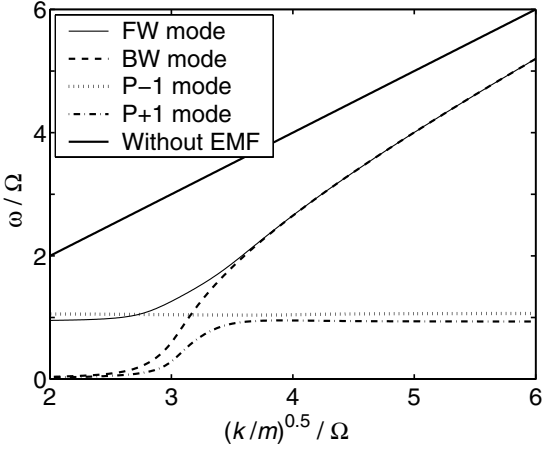


Figure 2. Frequencies of eigenvectors as function of shaft stiffness.

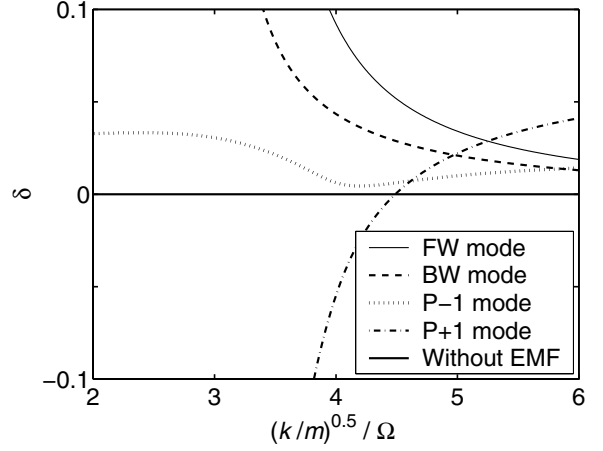


Figure 3. Decay constants of eigenvectors as function of shaft stiffness.

### 4.3 Vibration characteristics as function of shaft stiffness

Figure 2 and 3 show the frequencies and decay constants of the electromechanical rotor system without mechanical damping. For comparison, the rotor frequency is presented also without electromagnetic forces (EMF). Figure 2 shows that the whirling frequencies are somewhat lower than the fundamental frequency without electromechanical coupling. This results from the so-called negative-spring effect of electromagnetic forces. Further, the electromagnetic modes are independent of the shaft stiffness within high stiffness range.

As the shaft stiffness is decreased, the whirling modes and electromagnetic modes interact strongly with each other's. Figure 3 shows that the decay constants are all slightly positive within the high stiffness range. As the shaft stiffness is decreased, Mode  $p+1$  and therefore the whole system become unstable. The critical non-dimensional value for the shaft stiffness is  $\tilde{k} = 18.9$ . A more detailed study of the electromagnetic forces revealed that below this critical shaft stiffness, the electromagnetic forces feed energy into the whirling motion. In addition, it can be noted that the stiffness matrix  $\mathbf{K}$  is negative-definite when the shaft stiffness is less than the limit value  $\tilde{k} = 34.6$ .

### 4.4 Rotordynamic stability

Our system model is defined by 7 real valued parameters (Eq. 13 & 5). Figures 4 – 7 show four stability charts, in which three of the system parameters are varied and four held constant. The reference point for all the charts is defined by parameters:  $\tilde{k}_{p-1} = 0.1350$ ,  $\tilde{k}_{p+1} = 0.6442$ ,  $\tilde{a}_{p-1,Re} = -0.02$ ,  $\tilde{a}_{p+1,Re} = -0.0672$ ,  $\tilde{d} = 0.42$ , and  $s_0 = 0.032$ . The effective shaft stiffness  $\tilde{k}_e$  is varied in all figures.

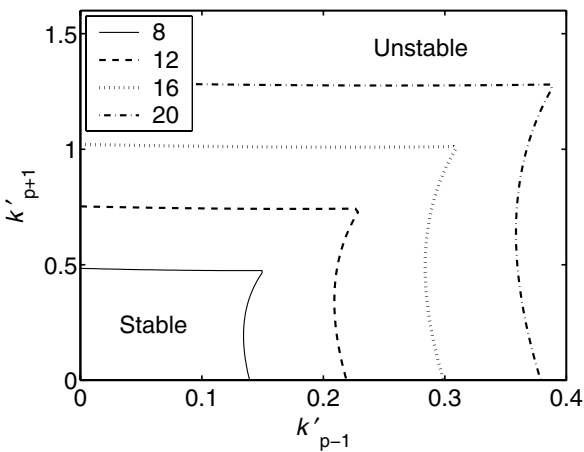


Figure 4. Stability borderlines for non-dimensional parameters  $k'_{p-1}$  ( $= \tilde{k}_{p-1}$ ),  $k'_{p+1}$  ( $= \tilde{k}_{p+1}$ ) and  $\tilde{k}_e$ .

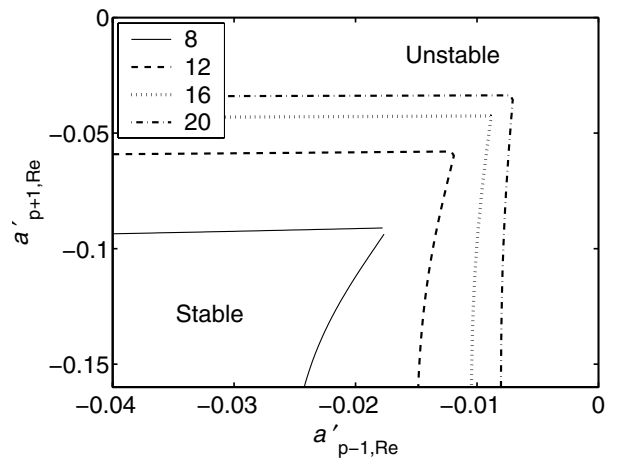


Figure 5. Stability borderlines for non-dimensional parameters  $a'_{p-1,Re}$  ( $= \tilde{a}_{p-1,Re}$ ),  $a'_{p+1,Re}$  ( $= \tilde{a}_{p+1,Re}$ ) and  $\tilde{k}_e$ .

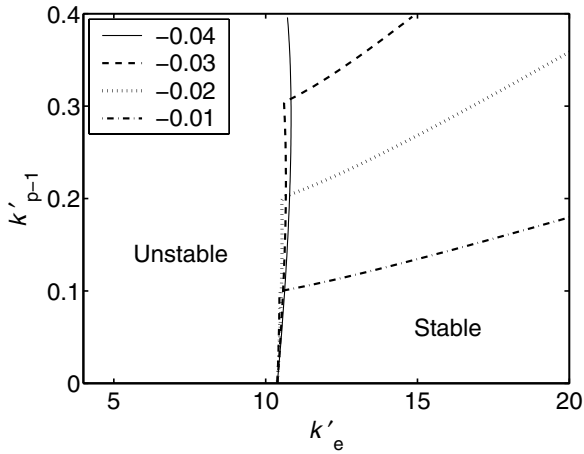


Figure 6. Stability borderlines for non-dimensional parameters  $k'_e (= \tilde{k}_e)$ ,  $k'_{p-1} (= \tilde{k}_{p-1})$  and  $\tilde{a}_{p-1,Re}$ .

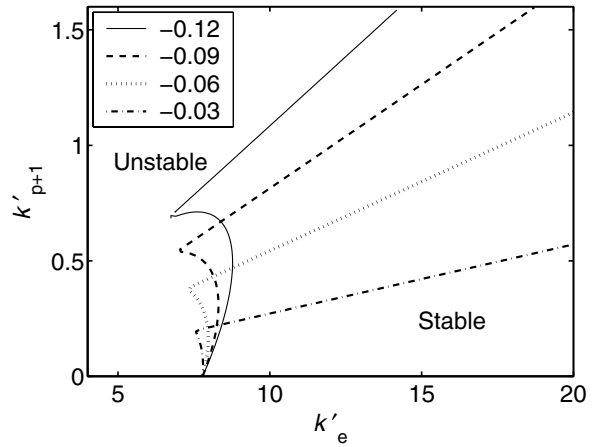


Figure 7. Stability borderlines for non-dimensional parameters  $k'_e (= \tilde{k}_e)$ ,  $k'_{p+1} (= \tilde{k}_{p+1})$  and  $\tilde{a}_{p+1,Re}$ .

Figures 4–7 show that the critical value of effective stiffness  $\tilde{k}_e$  depends clearly on the main system parameters. In addition, Figures 4 and 5 indicate that an increase of parameters  $\tilde{k}_{p\pm 1}$  and decrease of  $\tilde{a}_{p\pm 1,Re}$  may destabilize the system.

## 5. Discussion and conclusions

A simple electromechanical rotor model of an electric motor was generated. In addition to the Jeffcott rotor variable, the model included two additional complex variables describing the spatially linear effects of electromagnetic field. The obtained results confirm that the electromagnetic fields and the rotor vibrations may interact strongly. If the new electromagnetic variables are interpreted as ‘quasi-displacements’, the interaction turns up in the equations of motion as additional damping, stiffness and circulatory terms. The circulatory terms, i.e. cross-coupled stiffness terms, is a major source of instability in rotating machines. Thus, the presented model offers a new and simple explanation for electric motors, which is compatible with the experience of rotordynamic instabilities. The numerical example raised another explanation for rotordynamic instability. The system parameters may yield a negative-definite stiffness matrix (symmetric part), which destabilize the system without stabilizing forces. These explanations must be used as hypotheses for more detailed studies including the numerical simulation of electromechanical rotor systems and the validation procedures by experimental methods.

## 7. References

- [1] Früchtenicht J, Jordan H & Seinsch HO. (1982) Exzentrizitätsfelder als Ursache von Laufinstabilitäten bei Asynchronmaschinen, Teil I und II. *Arch. für Electrotechnik*, 65, 271–292.
- [2] Belmans R, Vandenput A & Geysen W. (1987) Calculation of the flux density and the unbalanced pull in two pole induction machines. *Arch. für Electrotechnik*, 70, 151–161.
- [3] Skubov D & Shumakovich IV. (1999) Stability of the rotor of an induction motor in the magnetic field of the current windings. *Mechanics of solids*, 34(4), 28–40. (Translated from *Mekhanika Tverdogo Tela*, 4, 36–50, 1999)
- [4] Arkkio A, Antila M, Pokki K, Simon A & Lantto E. (2000) Electromagnetic force on a whirling cage rotor. *IEE Proc.-Electr. Power Appl.*, 147, 353–360.
- [5] Parks PC & Hahn V. (1992) *Stability theory*. New York: Prentice-Hall.
- [6] Genta G. (1998) *Vibration of structures and machines. Practical aspects*. 3<sup>rd</sup> ed. New York: Springer-Verlag.
- [7] Ziegler H. (1968) *Principles of structural stability*. Waltham, Massachusetts: Blaisdell Publishing Company.
- [8] Vance JM (1987) *Rotordynamics of turbomachinery*. New York: John Wiley & Sons.
- [9] Bilharz H. (1944) Bemerkungen zu einem Satze von Hurwitz. *Z. angew. Math. Mech.*, 24, 77–82.

## Acknowledgments

The authors gratefully acknowledge the financial support of the National Technology Agency of Finland (Tekes). Special thanks are due to Dr. E. Lantto, High Speed Tech Ltd., and Mr. P. Klinge, VTT Industrial Systems, for valuable discussions.